

# Time Correlations in Mode Hopping of Coupled Oscillators

Mathias L. Heltberg<sup>1,2</sup> · Sandeep Krishna<sup>1,2</sup> ·  
Mogens H. Jensen<sup>1,2</sup>

Received: 6 December 2016 / Accepted: 16 February 2017 / Published online: 27 February 2017  
© Springer Science+Business Media New York 2017

**Abstract** We study the dynamics in a system of coupled oscillators when Arnold Tongues overlap. By varying the initial conditions, the deterministic system can be attracted to different limit cycles. Adding noise, the mode hopping between different states become a dominating part of the dynamics. We simplify the system through a Poincare section, and derive a 1D model to describe the dynamics. We explain that for some parameter values of the external oscillator, the time distribution of occupancy in a state is exponential and thus memoryless. In the general case, on the other hand, it is a sum of exponential distributions characteristic of a system with time correlations.

**Keywords** Coupled oscillators · Mode hopping · Arnold tongues · Poincare sections · Time correlations

## Introduction

Leo Kadanoff was a giant pioneer in the field of dynamical systems and chaos theory and was a fantastic inspiration for many of us collaborating with him over the years. With this paper we wish to honor the legacy of Leo by presenting a study of mode locking phenomena in a system with two characteristic frequencies, a topic that interested Leo for many years [1–5]. We analyse the hopping between limit cycles using Poincare sections, another topic that was of close interest to Leo.

Already in 1676, the dutch physicist Christian Huygens [6] observed that the dynamics of two coupled clocks resulted in synchronization [7]. This is one of the oldest non-linear phenomena ever to be described, and despite many attempts [8], the dynamics of a system

---

✉ Mogens H. Jensen  
mhjensen@nbi.ku.dk

<sup>1</sup> The Niels Bohr Institute, University of Copenhagen, København, Denmark

<sup>2</sup> Simons Centre for the Study of Living Machines, National Centre for Biological Sciences, Bangalore, India

of coupled oscillators is still far from completely understood. A classical example of this consists of two self-sustained oscillators where an external oscillator is weakly coupled to an internal oscillator. Systems of this character can show surprisingly complex behaviour [3,5], only parts of which are understood due to the pioneering work of Vladimir Arnold [9]: in regions called Arnold Tongues, these oscillators become synchronized, or entrained, to each other. In recent years, synchronization of coupled oscillators has been found in a variety of physical systems from fluids [2] to quantum mechanical devices [10,11], and during the last 10 years this has also been observed in many biological processes such as cell cycles [12–14], gene regulatory dynamics in synthetic populations [15], and protein oscillations in single cells [16], in particular oscillations in the transcription factor NF-κ B [17–20]. An important, but less well-understood, aspect is the dynamics in regions where two or more Arnold tongues overlap [21]. Here different synchronization are possible; mathematically, the trajectory in phase space can be attracted to different stable limit cycles depending on initial conditions.

### 1 Model of Protein Oscillations: Limit Cycles and Poincare Section

In this study we consider a network of 5 coupled differential equations, describing the dynamics of the important transcription factor NF-κ B, previously published in[22]. Here we consider the concentration of a molecule, that has a fixed concentration  $N_x$ , whose *active* form is described by  $x$ . This indirectly starts production of the molecule  $z$ , mediated through the variable  $y$ . As  $z$  increase the activation level of  $x$  decrease, leading to a negative feedback mechanism resulting in oscillations. A molecule, that has fixed concentration  $w$ , can assume three states,  $u$ ,  $v$  and  $w - u - v$  and the active form,  $u$ . It can lead to degradation of  $z$ , which again make  $x$  active. The activation of  $u$  is mediated by a periodically varying component, described by  $\tau$ . A schematic version of the network can be found in Fig. 1a. The equations now take the following form:

$$\begin{aligned} \dot{x} &= V_x(N_x - x) \frac{K_z}{K_z + z} - V_z \cdot z \frac{x}{K_x + x} \\ \dot{y} &= \Gamma_y x^2 - \Delta_y y \\ \dot{z} &= \Gamma_z \cdot y - \Delta_z \cdot u \cdot (N_x - x) \frac{z}{K_z + z} \\ \dot{u} &= \Gamma_u \cdot \tau \cdot w - \Delta_u \cdot u \\ \dot{v} &= \Gamma_v \cdot u - V_v \cdot v \frac{K_A}{K_A + A_{20}\tau} \\ \tau &= 0.5 + A \sin\left(\frac{2\pi}{T} t\right) \\ w &= N_{uv} - u - v \end{aligned}$$

Here all the capital letters refer to fixed parameters of the model, whereas lowercase letters refer to variables.

In order to study the system, we define a Poincare section at  $x = 1500$  allowing us to perform discrete analysis on the 4 other variables and the time of each period [23]. For a set of external parameters corresponding to a region where two Arnold Tongues overlap, we find that the deterministic system can settle into different limit cycles (Fig. 1b), where typically the period of the internal oscillator is an integer times the period of the

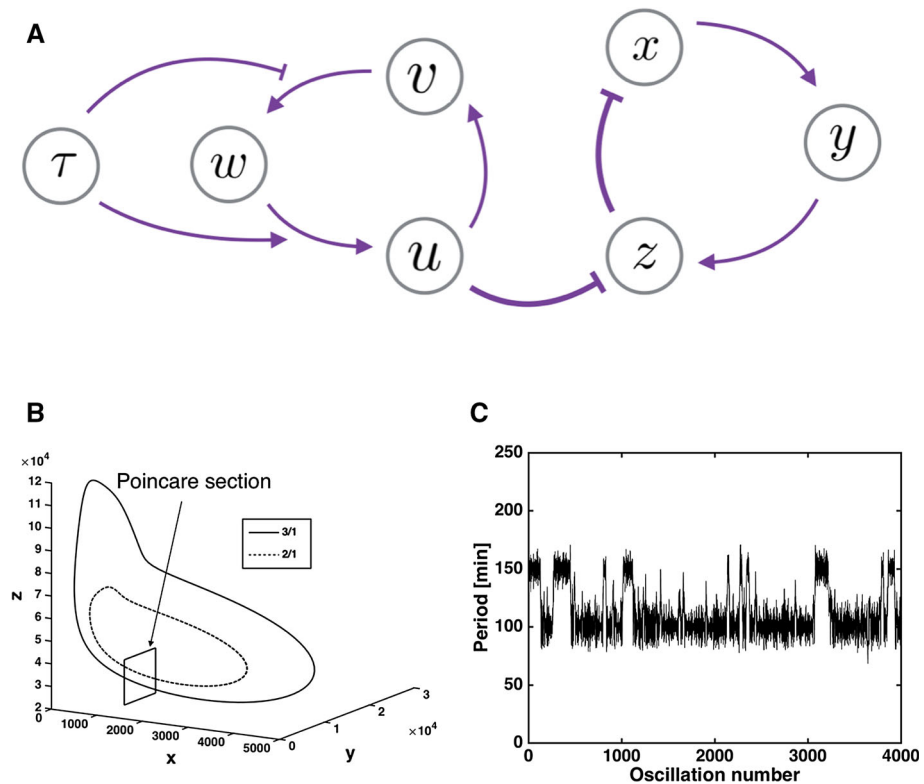


**Fig. 1** **a** Schematic figure showing the network, that give rise to the equations in the model. **b** The two stable limit cycles for the deterministic system with external oscillator parameters  $T = 50$  min and  $A = 0.1$ . Shown here is the phase space of variables  $x$ ,  $y$ , and  $z$ , and the Poincaré section we use in our analysis. **c** Fluctuations in the time period for this system in the presence of noise; external oscillator parameters are  $T = 50$  min and  $A = 0.1$

external oscillator (in principle other limit cycles exist, but it is harder to find the initial conditions and parameter values that produce them). Dynamical systems of multi-stability have been studied in many aspects [24,25], usually through the coupling of separate attractors, but the arise of multi-stability through the overlapping of Arnold tongues, has not been thoroughly investigated and serve as an interesting system to study the appearance and disappearance of different stable limit-cycles. Interestingly, we find that when we add noise to the system (by using the Gillespie algorithm to simulate the system [26]), transitions between these co-existing limit cycles is observed (Fig. 1c). This phenomena we describe as *mode hopping*, reflecting that the trajectory inside the Poincaré section hops between different entrainment modes. Our goal is to describe the time correlations between transitions in this system with a discrete time model, using information extracted from the Poincaré section. Transitions are of course only possible when noise is added to the system. The noise makes it difficult to determine every transition with complete precision, but combining studies of the deterministic system with sufficiently long stochastic time-series to generate enough statistics, we will be able to make conclusions about the nature of these transitions.

## Distribution of Noise in the Poincare Section

We begin by studying the distribution of positions on the Poincare section after precisely one period of oscillation, where all trajectories started at the same initial point in the Poincare section. Mathematically speaking we want to find the distribution  $P(x_i^n | x_i^{n-1} = \mu_i)$ , where  $x_i^n$  is the position of the  $i$ th variable on the Poincare section after  $n$  periods of the oscillation, given that the position in the Poincare section after  $n - 1$  oscillations was  $\mu_i$  (the period is also regarded as a variable). From our simulations, we find that, independent of the starting position  $\mu_i$ , the distribution of time period of the oscillation is Gaussian (Fig. 2a), and that its standard deviation,  $\sigma$ , to a good approximation, can be treated as constant (Fig. 2b). Furthermore, we observed the same for every other variable and thus, to a good approximation, we can describe  $P$  as a multivariate Gaussian:

$$P(\mathbf{x} | \mathbf{x}_0 = \boldsymbol{\mu}) = \frac{1}{\sqrt{2\pi}^5 \sqrt{|V|}} e^{-\frac{1}{2} [(\bar{x} - \bar{\mu}) V^{-1} (\mathbf{x} - \boldsymbol{\mu})]}$$

Thus, within the Poincare section, the system can be described as a deterministic trajectory with Gaussian noise. This observation is of great importance, and to use this further, we study how a trajectory with initial position perturbed from the limit cycle, is attracted to the given limit cycle within the Poincare section, which in general depends on the possibly complex geometry of the basin of attraction of the limit cycle. We first consider the absolute value of the difference between the period and the period of the previous oscillation in deterministic simulations. We find that this quantity exhibits a complicated structure, but overall goes to zero with an exponential decay as the limit cycle is approached (Fig. 2c, d). We find that independent of the initial condition, but for fixed parameters of the external oscillator, the exponential decay has the same decay constant, that changes slightly, as the external parameters change (Fig. 2c, d). The non-smooth structure arises from the coupling between variables and is reminiscent of a damped harmonic oscillator, but in our subsequent analysis we will treat this as a negligible effect on top of the basic exponential decay characteristic to each basin of attraction.

To finish the description, we must locate the boundary between each basin of attraction. Starting from various initial conditions, we need to map which limit cycle each initial conditions settles into. In order to choose sensible initial positions, we take  $10^4$  recorded points from a stochastic simulation, and use these as initial conditions. After 10 oscillations, we find that the majority have settled into one of the two limit cycles, but some are still unsettled (Fig. 2e). This seems to be a result of an unstable  $5/2$  Arnold tongue. We note importantly that the basins are not riddled, but to good approximation can be regarded as divided in groups. To simplify this we consider the shortest distance between the two stable limit cycles in the Poincare section, and consider the points in between as initial conditions. Figure 2f shows that after 40 oscillations, all trajectories have settled into one of the two stable limit cycles, and that as we increase the amplitude of the external oscillator, the basin of attraction for one basin grows, whereas the other decreases. Thus, for a given set of external parameters, we can approximate the width of the basin of attraction compared to the standard deviation of the Gaussian noise. Changing the amplitude of the external oscillator would change the probability to be in one of the limit cycles for the stochastic system and thus change the average number of oscillations before leaving the given entrained state.

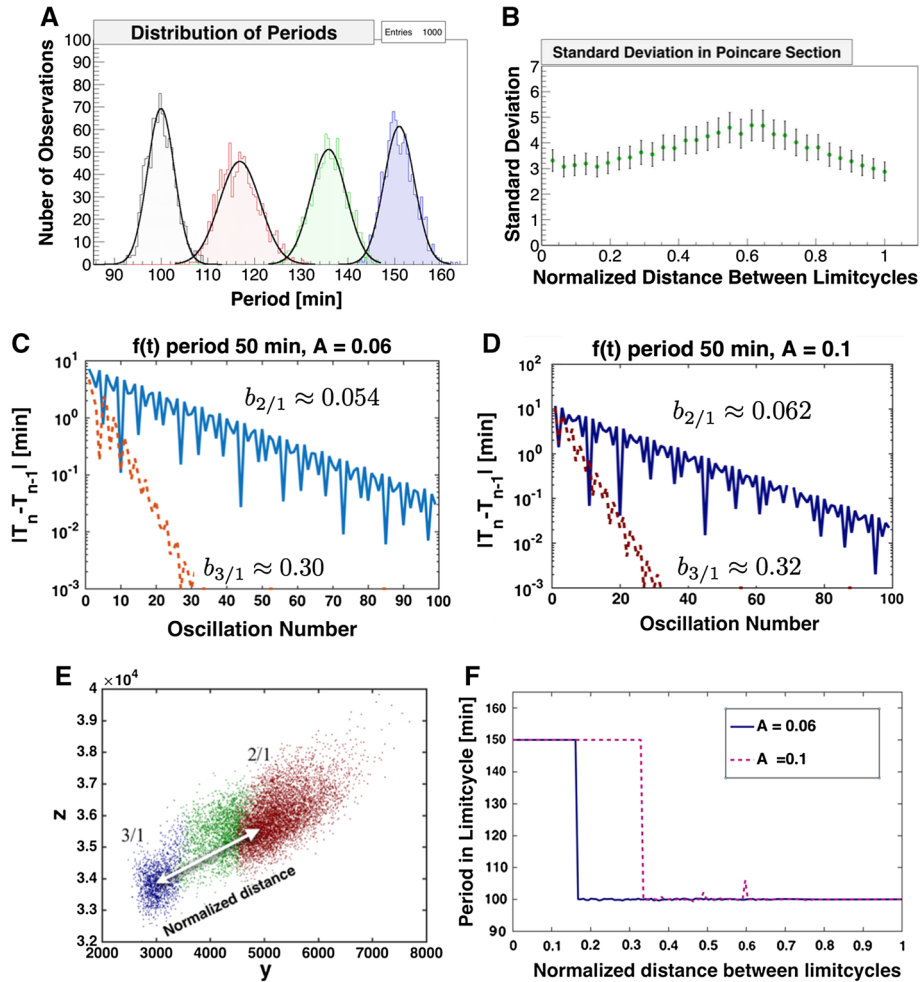


**Fig. 2** **a** Gaussian fits for the distribution of periods after one trajectory started at 4 different initial positions in the Poincare section. **b** Value of the standard deviation of the Gaussian fit at different positions in the Poincare section. The normalized distance is here defined as the norm of a vector from the position in phase space of one limit cycle to the other limit cycle, when they intersect with the Poincare section. **c**, **d** Absolute value difference between period and previous period, as the trajectories decay into the limit cycle. The parameter  $b$  is the exponential decay constant. **e**  $10^4$  points from stochastic simulation used as initial values for deterministic simulation. After 10 oscillations *blue* has period greater than 145 min and *red* has period smaller than 105 min. *Green* refers to points between these values. **f** Width of the basin of attraction for different values of the amplitude of the external oscillator after 40 oscillations

## A Model for the Dynamics in the Poincare Section

At this point we have argued that for a fixed set of parameters of the external oscillator, the decay into a limit cycle for the internal oscillator follows exponential decay with a constant depending on the basin of attraction. Secondly, the boundaries, and therefore width, of this basin are determined by the external parameters. Thirdly, the next position in phase space

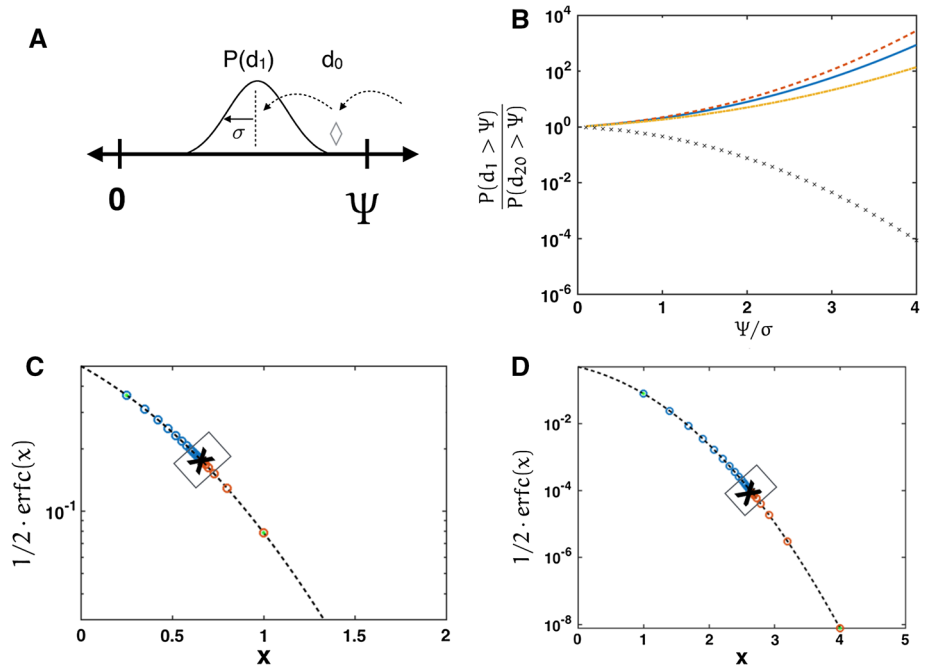


**Fig. 3** **a** Schematic cartoon of the 1D model. **b** Ratio between the probability to leave the state after the first jump and after 20 jumps (in steady state), plotted for the different parameters and initial positions in the model. **c** The probability to leave the state, plotted on the error function. *Orange* starting from  $d_0 = 0$  and *blue* starting from  $d_0 = \Psi$ .  $\Psi/\sigma = 1$ . The *cross* indicates the steady state. **d** The probability to leave the state, plotted on the error function. *Orange* starting from  $d_0 = 0$  and *blue* starting from  $d_0 = \Psi$ .  $\Psi/\sigma = 4$ . The *cross* indicates the steady state.

inside the Poincare section is Gaussian distributed with a characteristic standard deviation determined by the noise in the system.

From these results, we thus create a simple, discrete 1D model, that should be able to qualitatively explain the results we find for the dynamics for the stochastic system. We imagine a measure,  $d_n$ , that defines the distance to the center of the limitcycle inside a given basin of attraction. We consider the 1D map:

$$d_n = d_{n-1}\Delta = d_0\Delta^n = d_0e^{ln(\Delta)n} \tag{1.1}$$

Now we add Gaussian noise to the system, so the update is:

$$d_n = d_{n-1}\Delta + \mathcal{N}(0, \sigma) = \mathcal{N}(d_{n-1}\Delta, \sigma), \tag{1.2}$$

where  $\mathcal{N}$  defines the normal distribution with parameters given in the argument. A schematic version of this simple model, is shown in Fig. 3a. We are now interested in knowing the probability density function,  $P(d_n)$ . This can thus be described as:

$$P(d_n) = P(d_n|d_{n-1})P(d_{n-1}) \tag{1.3}$$

We start by considering the position after one jump, given the initial position is  $d_0$ , described by:

$$P(d_1) = \frac{1}{\sqrt{2\pi}\sigma} e^{-\frac{1}{2}\left(\frac{d_1 - \Delta d_0}{\sigma}\right)^2}$$

Now we want to calculate the distribution for the position after the second step. To calculate this we are thus (to avoid too many  $ds$  we define  $d = d_0$ ,  $y = d_1$  and  $x = d_2$ ) solving the integral:

$$\begin{aligned} P(x) &= \frac{1}{\sqrt{2\pi}\sigma_1\sigma_2} \int_{-\infty}^{\infty} e^{-\frac{1}{2}\left(\frac{x-\Delta y}{\sigma_1}\right)^2} e^{-\frac{1}{2}\left(\frac{y-\Delta d}{\sigma_2}\right)^2} dy \\ &= \mathcal{N}\left(\Delta^2 d, \sqrt{\sigma_1^2 + \sigma_2^2 \Delta^2}\right). \end{aligned}$$

As this holds for every step, we can iterate from the first jump  $d_1$ . That is, the PDF of the  $n$ th jump becomes:

$$P(d_n) = \frac{1}{\sqrt{2\pi}\sigma_n} e^{-\frac{1}{2}\left(\frac{d_n - \Delta^n d_0}{\sigma_n}\right)^2}$$

where  $\sigma_n = \sigma \sqrt{\sum_{i=0}^{n-1} \Delta^{2i}} = \sigma \sqrt{\frac{1 - \Delta^{2n}}{1 - \Delta^2}}$ .

Now in order to consider transitions between basins of attraction, we must consider the probability that the distance  $d$  is larger than the boundary of the basin, defined as  $\Psi$ . Thus:

$$\begin{aligned} P(d_n > \Psi) &= \int_{\Psi}^{\infty} \frac{1}{\sqrt{2\pi}\sigma_n} e^{-\frac{1}{2}\left(\frac{x - \Delta^n d_0}{\sigma_n}\right)^2} dx \\ &= \frac{1}{2} \operatorname{erfc}\left(\frac{\Psi - \Delta^n d_0}{\sigma_n}\right) \end{aligned}$$

From this we can also see that this will always reach a steady state, where the probability of leaving (i.e., a transition out of the basin of attraction) will be:

$$\begin{aligned} \lim_{n \rightarrow \infty} P(d_n > \Psi) &= \lim_{n \rightarrow \infty} \left( \frac{1}{2} \left[ \operatorname{erfc}\left(\frac{\Psi - \Delta^n d_0}{\sigma_n}\right) \right] \right) \\ &= \frac{1}{2} \left[ \operatorname{erfc}\left(\frac{\Psi}{\sigma} \sqrt{1 - \Delta^2}\right) \right] \end{aligned}$$

This means that the probability of leaving will, in steady state, be highly dependent on the relation between  $\Psi$  and  $\sigma$ , but independent of the initial position  $d_0$ . The probability to leave the state in the first jump, however, will always be dependent on the initial position. If we assume  $d_0 = \Psi$  we obtain:

$$P(d_1 > \Psi | d_0 = \Psi) = \frac{1}{2} \left[ \operatorname{erfc}\left(\frac{\Psi}{\sigma} (1 - \Delta)\right) \right],$$

which shows that the probability to leave in the first jump is higher than in the steady state. If we consider  $d_0 = 0$  we obtain:

$$P(d_1 > \Psi | d_0 = 0) = \frac{1}{2} \left[ \operatorname{erfc} \left( \frac{\Psi}{\sigma} \right) \right],$$

which shows that the probability to leave in the first jump is lower than in the steady state.

With these results, we have an interesting measure, the ratio between the probability of leaving in the first iteration, divided by the probability of leaving in the steady state. This ratio is plotted in Fig. 3b for different values of  $\Delta$  and different initial positions. Another visualization of this is the probability to leave for each step, depending on the initial condition, for  $\Psi/\sigma = 1$  (Fig. 3c) and for  $\Psi/\sigma = 4$  (Fig. 3d).

We now proceed to calculate the probability distribution for the first time to leave the entrained state,  $J_1$ , meaning the first time the distance will be greater than  $\Psi$ :

$$P(J_1 = n) = \frac{1}{2^n} \left[ 1 - \operatorname{erf} \left( \frac{\Psi - \Delta^n d_0}{\sigma_n} \right) \right] \prod_{j=1}^{n-1} \operatorname{erf} \left( \frac{\Psi - \Delta^j d_0}{\sigma_j} \right). \tag{1.4}$$

Assuming that  $d_0 = \Psi$  we can reduce the above expression:

$$P(J_1 = n | d_0 = \Psi) = \tag{1.5}$$

$$\frac{1}{2^n} \operatorname{erfc} \left( \frac{\Psi}{\sigma} \sqrt{1 - \Delta^2} \sqrt{\frac{1 - \Delta^n}{1 + \Delta^n}} \right) \prod_{j=1}^{n-1} \operatorname{erf} \left( \frac{\Psi}{\sigma} \sqrt{1 - \Delta^2} \sqrt{\frac{1 - \Delta^j}{1 + \Delta^j}} \right). \tag{1.6}$$

From this expression, it should be deduced, that the argument depending on  $n$  will converge to one, meaning that the probability to jump out will quickly reach a steady state. In the steady state there is always the same probability to jump out, and the distribution describing a discrete event with the same probability will be the exponential distribution.

### Approximation to the Distribution

As we observed in the above expressions and in Fig. 3c, b, it takes several iterations to reach the steady state, and we expect that these initial probabilities can be described by a single exponential distribution. Therefore, we expect that the distribution of oscillations in one limit cycle before transition, can be described by a sum of two exponential distributions:

$$f(n) = \overset{\text{Initialposition}}{A e^{-bn}} + \overset{\text{SteadyState}}{C e^{-dn}}$$

where  $n \equiv d_n > \Psi \wedge d_{n-1}..d_1 \leq \Psi$ .

Testing this assumption, we now try to compare simulations on the 1D model with the real system. For both systems we start at  $d_0 = \Psi$ , i.e., on the border of the basin of attraction, defined from the normalized distance between the limit cycles (Fig. 4a, b), and at  $d_0 = 0$ , i.e., at the center of the limit cycle (Fig. 4c, d). In these simulations, we define that the trajectory leaves the entrained state when the period becomes closer to the period in the other limit cycle. Even though these simulations cannot be compared quantitatively, since the 1D model does not take the cycles of the decay into account, they do have the same qualitative description of the dependence on initial positions, and are well described by the suggested function. The interpretation of the above result is as follows: The first several oscillations follows a distribution of either decreasing (if  $d_0 = \Psi$ ) or increasing (if  $d_0 = 0$ ) probability of transition out of the entrained state, before reaching the steady state probability. In the steady state, this should follow an exponential distribution since there is at each iteration the

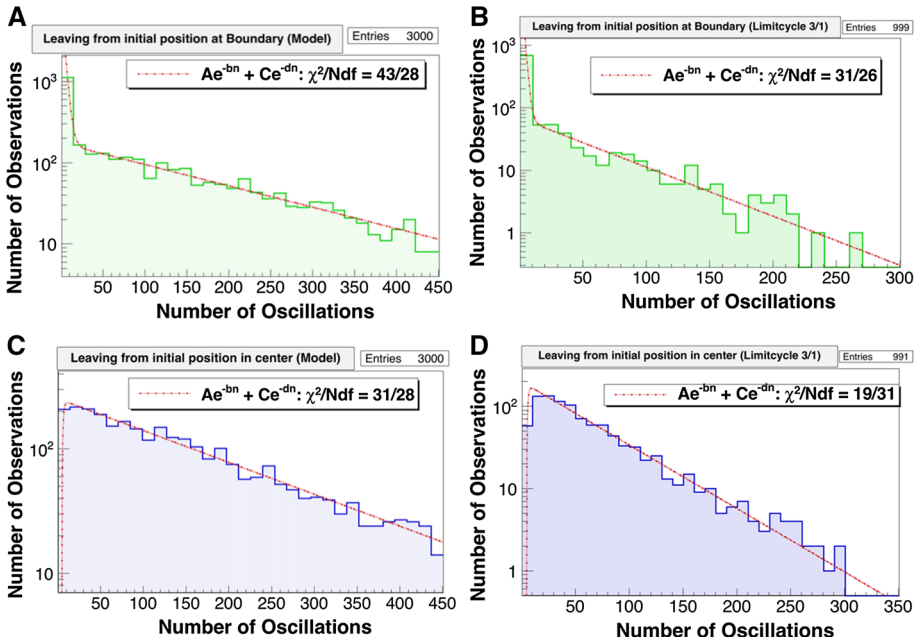


**Fig. 4** **a** Distribution of number of jumps before leaving the state for the model. Initial position  $d_0 = \Psi$ . **b** Distribution of number of jumps before leaving the state for the simulated system. Initial position around the boundary. **c** Distribution of number of jumps before leaving the state for the model. Initial position  $d_0 = 0$ . **d** Distribution of number of jumps before leaving the state for the simulated system. Initial position in the center of the limit cycle

same probability to leave, which can be seen from the fact that the exponential decay, if the first fraction of the plot is neglected, has exactly the same slope independent of the initial position. However, the effect of the initial effect conditions is captured in the first part of the fit, where we find that these effects can be estimated by adding another exponential function.

### Long Time Dynamics

Now we want to study the long term dynamics, and estimate the distribution of number of oscillations in one limit cycle, before leaving the limit cycle. As seen in Fig. 1b, there clearly are transitions between states, but to define exactly when the trajectory is out of the basin of attraction of a specific limit cycle can be difficult. We here use Fisher’s discriminant, implemented in MATLAB, to separate the points, and classify them between different states [27]. From the model we expect the distribution to reach a steady state after some trajectories in the same limit cycle, but having much higher probability to leave the state in the early rounds, as we usually enter a new state close to the boundary. We again expect the distribution to fit the sum of two exponentials, where the first position in the basin of attraction follows a distribution but is always close to the boundary of the basin. This is confirmed in Fig. 5a, where we have also plotted the best exponential and stretched exponential fit. From Fig. 4b the other limit cycle in this experiment also follows the sum of two exponentials, and that this state is a little different from the one shown in 5A, due to the  $\Delta$  of this state is higher.

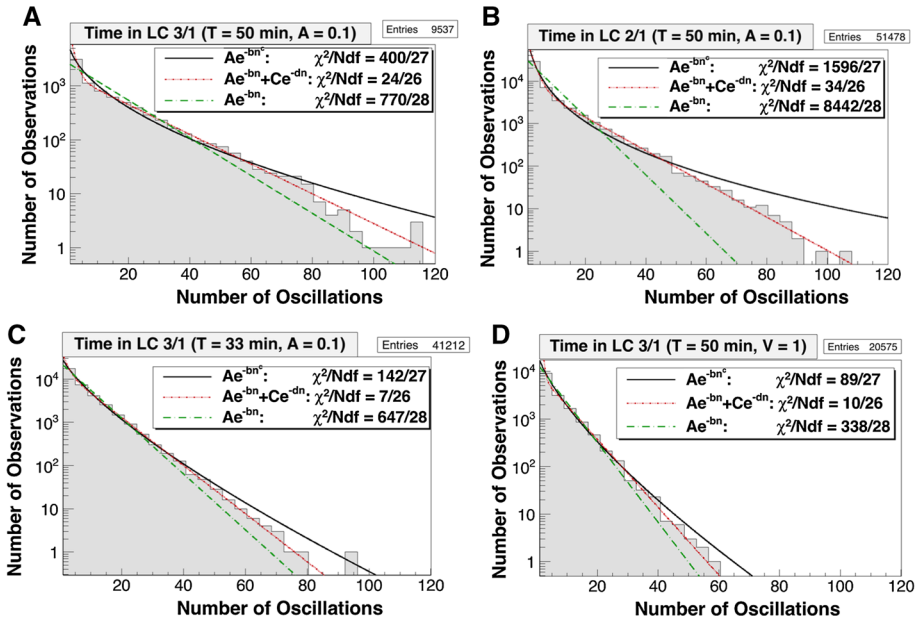


**Fig. 5** **a** Distribution of oscillations in 3/1 state for totally 600000 oscillations. Parameters of external oscillator is T = 50 min and A = 0.1. V = 2 · 10<sup>-14</sup>L. **b** Distribution of periods for the 2/1 limit cycle. From the model perspective this distribution is different from **a** in the value of Δ. Same parameters used. **c** Distribution of oscillations in 3/1 limit cycle. for external parameters T = 33 min and A = 0.1. **d** Distribution of periods for the 3/1 limit cycle. Parameters of external oscillator is T = 50 min and A = 0.1. V = 1 · 10<sup>-14</sup>L

Now if the value of  $\Psi/\sigma$  can be estimated to be small, the effective dynamics is however imagined to be closer to an exponential distribution as the ratio shown in Fig. 3b gets smaller. Now from the model we estimate that we would have more exponential like fits, if we:

- (a) Decreased external period (causing smaller  $\Psi$ )
- (b) Decreased external amplitude (causing smaller  $\Psi$ )
- (c) Decreased Volume = Larger noise (causing larger  $\sigma$ )

Lowering the amplitude of the external oscillator, effectively decreases the distance between the two limit cycles and transitions between limit cycles should be more frequent, as the noise level remains constant. This prediction is confirmed in Fig. 5c where the probability of leaving the limit cycle in the steady state is higher than in Fig. 5a, b. Also we note that this distribution is much closer to being exponential than the figures above, which was predicted by the results in Fig. 3. In the same manner we expect that if we keep the width of the basin constant, meaning we fix the parameters of the external oscillator, but we add more noise to the system, similar effects should be observed. In Fig. 5d we see that if we increase the noise of the system, the probability to leave the state increases in the steady state, and the distribution is again closer to an exponential distribution than before. This means that we have obtained an understanding, not only of why the distribution of time in one state follows two exponentials, but also how the parameters in this distribution change, as we change the external parameters.

## Conclusion

We have shown how the dynamics of a system of coupled oscillators, in the overlapping Arnold Tongue regime, can show bistable behaviour, and how the statistics for the transitions between limit cycles can be controlled by changing the parameters of the external oscillator. We have observed how the distribution of the number of oscillations in each state tends to look exponential in some parameter ranges, while in others looks very stretched. We showed that this behaviour is reproduced in a simple 1D system, derived from the behaviour within Poincare section of the system, leading us to a useful description of the dynamics as a sum of two exponential functions. We believe that these results can be used to describe the dynamics of many synchronized oscillating systems in the presence of noise, even when the basins of attraction are divided by several regions.

**Acknowledgements** SK thanks the Simons Foundation for funding. MLH and MHJ acknowledge support from the Danish Council for Independent Research and Danish National Research Foundation through Stem-Phys Center of Excellence, grant number DNR116.

## Appendix A

### Description of the biological model

The network of the transcription factor NF-κB is very important for the mammalian protein production, and several models have therefore been constructed to capture the essential dynamics

Here we use the NF-κB model, published in 2012 by Jensen and Krishna. In this model, we consider the NF-κB inside the nucleus, acting as a transcription factor for a great variety of different proteins, including I-κB. This forms a complex with NF-κB, making it unable to enter the nucleus, which means it is inactive. In order to create a time delay, the equation for the I-κB RNA is added, which gives a three node network. Now we consider the protein complex IKK, that can phosphorylate the NF-κB - I-κB complex and thus make NF-κB active again. We assume that there IKK can be in three states: active, neutral and inactive. Furthermore we assume that is a finite amount of both NF-κB and I-κB, but nothing is spontaneously degraded. With these assumptions at hand, we describe the system by the five coupled differential equations:

$$\begin{aligned} \dot{N}_n &= k_{Nin}(N_{tot} - N_n) \frac{K_I}{K_I + I} - k_{Iin}I \frac{N_n}{K_N + N_n} \\ \dot{I}_{RNA} &= k_t N_n^2 - \gamma_m I_{RNA} \\ \dot{I} &= k_{tI} I_{RNA} - \alpha I K K_a (N_{tot} - N_n) \frac{I}{K_I + I} \\ \dot{I} K K_a &= k_a f(t) ([I K K]_{tot} - I K K_a - I K K_i) - k_i I K K_a \\ \dot{I} K K_i &= k_i I K K_a - k_p I K K_i \frac{k_{A20}}{k_{A20} + [A20] f(t)} \\ f(t) &= 0.5 + A \sin\left(\frac{2\pi}{T} t\right) \end{aligned}$$

The parameters in the mode can be seen in the Table 1.

**Table 1** Default values of parameters in the model.  $[I K K]_{tot}$  and  $[A20]$  were chosen in order to obtain sustained spiky oscillations with frequency in the range  $0.3\text{--}1\text{ hr}^{-1}$  when  $[TNF]$  is kept fixed at 0.5 (the actual frequency obtained with these values is  $\nu_0 = 1/1.8\text{ hr}^{-1}$ )

Original parameter	Parameter in paper	Default value
$k_{Nin}$	$V_x$	$5.4\text{ min}^{-1}$
$k_{Iin}$	$V_z$	$0.018\text{ min}^{-1}$
$k_t$	$\Gamma_y$	$1.03(\mu\text{M})^{-1}\cdot\text{min}^{-1}$
$k_{tl}$	$\Gamma_z$	$0.24\text{ min}^{-1}$
$K_I$	$K_z$	$0.035\ \mu\text{M}$
$K_N$	$K_x$	$0.029\ \mu\text{M}$
$\gamma_m$	$\Delta_y$	$0.017\text{ min}^{-1}$
$\alpha$	$\Delta_z$	$1.05(\mu\text{M})^{-1}\cdot\text{min}^{-1}$
$N_{tot}$	$N_x$	$1.\ \mu\text{M}$
$k_a$	$\Gamma_u$	$0.24\text{ min}^{-1}$
$k_i$	$\Delta_u$	$0.18\text{ min}^{-1}$
$k_p$	$V_v$	$0.036\text{ min}^{-1}$
$k_{A20}$	$K_A$	$0.0018\ \mu\text{M}$
$[I K K]_{tot}$	$w$	$2.0\ \mu\text{M}$
$[A20]$	$A_{20}$	$0.0026\ \mu\text{M}$

## Appendix B

### Implementation of Gillespie algorithm

In the Gillespie algorithm we consider a volume  $V$ , with a spatially uniform mixture of  $N$  chemical species that can react through  $M$  different reactions,  $R_1 \dots R_M$ . The number of each of the species is denoted  $X_1 \dots X_N$ . At  $t = 0$ , we thus consider the initial number of molecules and calculates all reactions. The first goal is now to calculate the PDF, for the time until the next reaction occur

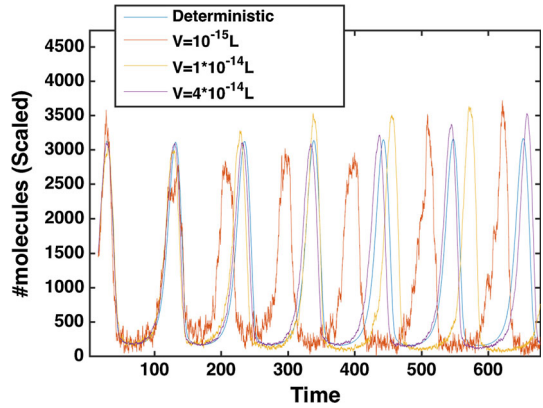
We consider the probability that the next reaction is of type  $\epsilon$ , and it occurs in the time-interval  $[t + \tau, t + \tau + dt]$ . We therefore consider:

$$P(\tau, \epsilon)d\tau = \frac{\text{No reaction in } [t, t+\tau]}{P_{not}(\tau)} \cdot \frac{\text{Reaction } \epsilon \text{ occurs}}{R_\epsilon d\tau}$$

Therefore we want to describe  $P_{not}(\tau)$  in terms of the rates. Since at each timestep  $\epsilon$ , the probability for no reaction to appear is:

$$P_{not}(dt) = 1 - \sum_{i=1}^N R_i dt$$

**Fig. 6** Trajectories starting from the same initial conditions for different noise levels. Here oscillations are shown in the variable  $x$



We can thus define  $\tau \equiv n \cdot dt$  and then:

$$P_{not}(\tau) = P_{not}(dt)^n = \left( 1 - \sum_{i=1}^N R_i \frac{\tau}{n} \right)^n = e^{-r\tau}$$

where  $r \equiv \sum_{i=1}^N R_i$

This means that we should generate a random number according to the exponential distribution, and a random number according to a uniform distribution. Here we can use the transformation method, and we can then create the update process, where at each step we jump a step in time  $\tau$  to next reaction, and picks the reaction according to  $r$ . Schematically the Gillespie algorithm can be described as:

- Pick two random numbers,  $v_1$  and  $v_2$ . Calculate time until next reaction:

$$\tau = -\frac{\ln(v_1)}{r}$$

Pick the next reaction:

$$\epsilon = \frac{\sum_{i=1}^{k-1} r_i}{\sum_{j=1}^n r_j} < v_2 \leq \frac{\sum_{i=1}^k r_i}{\sum_{j=1}^n r_j}$$

- Update the system according to the chosen reaction.

In this way the system can be updated, and adjusting the reactions to each time step. As can be seen in Fig. 6, changing the volume, changes the noise level, since we have two fixed concentrations in the model and therefore the considered number of molecules change. In the limit of a high number of molecules, this should be very close to deterministic.

## References

1. Jensen, M.H., Kadanoff, L.P., Krishna, S.: Universal behaviour of coupled oscillators: lessons for biology preprint (2016)
2. Stavans, J., Heslot, F., Libchaber, A.: Fixed winding number and the quasiperiodic route to chaos in a convective fluid. Phys. Rev. Lett. **55**, 596–599 (1985)

3. Jensen, M.H., Bak, P., Bohr, T.: Complete devil's staircase, fractal dimension and universality of mode-locking structure in the circle map. *Phys. Rev. Lett.* **50**, 1637–1639 (1983)
4. Jensen, M.H., Kadanoff, L.P., Libchaber, A., Procaccia, I., Stavans, J.: Global universality at the onset of Chaos: results of a forced Rayleigh Benard experiment. *Phys. Rev. Lett.* **55**, 2798–2801 (1985)
5. Jensen, M.H., Bak, P., Bohr, T.: Transition to chaos by interaction of resonances in dissipative systems. I. Circle maps. *Phys. Rev. A* **30**, 1960–1969 (1984)
6. Huygens, C.: A copy of the letter on this topic to the Royal Society of London appears in 1893. In: Nijhoff, M. (ed.) *Oeuvres Completes de Christian Huygens*, vol. 5, p. 246. Societe Hollandaise des Sciences, The Hague (1989)
7. Pikovsky, A., Rosenblum, M., Kurths, J.: *Synchronization: A Universal Concept in Nonlinear Sciences*. Cambridge University Press, Cambridge (2003)
8. Ramirez, J.P., Olvera, L.A., Nijmeijer, H., Alvarez, J.: The sympathy of two pendulum clocks: beyond Huygens' observations. *Sci. Rep.* **6**, 23580 (2016)
9. Arnold, V.I., Avez, A.: *Ergodic Problems of Classical Mechanics*. Addison-Wesley, Boston (1989)
10. Brown, S.E., Mozurkewich, G., Gruner, G.: Subharmonic shapiro steps and devil's-staircase behavior in driven charge-density-wave systems. *Phys. Rev. Lett.* **52**, 2277–2380 (1984)
11. Gwinn, E.G., Westervelt, R.M.: Frequency Locking, quasiperiodicity, and Chaos in Extrinsic Ge. *Phys. Rev. Lett.* **57**, 1060–1063 (1986)
12. Tsai, T.Y., Choi, Y.S., Ma, W., Pomerening, J.R., Tang, C., Ferrell Jr., J.E.: Robust, tunable biological oscillations from interlinked positive and negative feedback loops. *Science* **321**, 126–129 (2008)
13. Goldbeter, A.: Computational approaches to cellular rhythms". *Nature* **420**, 238–245 (2002)
14. Woller, A., Duez, H., Staels, B., Lefranc, M.: A mathematical model of the liver circadian clock linking feeding and fasting cycles to clock function. *Cell Rep.* **17**, 1087–1097 (2016)
15. Mondragon-Palomino, O., Danino, T., Selimkhanov, J., Tsimring, L., Hasty, J.: Entrainment of a population of synthetic genetic oscillators. *Science* **333**, 1315–1319 (2011)
16. Mengel, B., Hunziker, A., Pedersen, L., Trusina, A., Jensen, M.H., Krishna, S.: Modeling oscillatory control in NF- $\kappa$ B, p53 and Wnt signaling. *Curr. Opin. Genet. Dev.* **20**, 656–664 (2010)
17. Hoffmann, A., Levchenko, A., Scott, M.L., Baltimore, D.: The I $\kappa$ B-NF- $\kappa$ B signaling module: temporal control and selective gene activation. *Science* **298**, 1241–1245 (2002)
18. Nelson, D.E., et al.: Oscillations in nf- $\kappa$ b signaling control the dynamics of gene expression. *Science* **306**, 704–708 (2004)
19. Krishna, S., Jensen, M.H., Sneppen, K.: Spiky oscillations in NF-kappaB signalling. *Proc. Natl. Acad. Sci.* **103**, 10840–10845 (2006)
20. Tay, S., Kellogg, R.: Noise facilitates transcriptional control under dynamic inputs. *Cell* **160**, 381–392 (2015)
21. Heltberg, M.L., Kellogg, R.A., Krishna, S., Tay, S., Jensen, M.H.: Noise induces hopping between NF- $\kappa$ B entrainment modes, *Cell Syst.* (2016)
22. Jensen, M.H., Krishna, S.: Inducing phase-locking and chaos in cellular oscillators by modulating the driving stimuli. *FEBS Lett.* **586**, 1664–1668 (2012)
23. Strogatz, S.H.: *Dynamical Systems and Chaos*, pp. 278–279. Westview Press, Cambridge (2000)
24. Sun, H., Scott, S.K., Showalter, K.: Uncertain destination dynamics. *Phys. Rev. E* **60**(4), 3876 (1999)
25. Hens, C., Dana, S.K., Feudel, U.: Extreme multistability: Attractor manipulation and robustness. *Chaos* **25**(5) (2015)
26. Gillespie, D.T.: Exact stochastic simulation of coupled chemical reactions. *J. Phys. Chem.* **81**(25), 2340–2361 (1977). doi:[10.1021/j100540a008](https://doi.org/10.1021/j100540a008)
27. Fisher, R.A.: The use of multiple measurements in taxonomic problems. *Ann. Eugen.* **7**, 179–188 (1936)